19th Brazilian Congress of Thermal Sciences and Engineering
November 06th-10th, 2022, Bento Gonçalves - RS - Brazil

ENCIT2022-0077
ELECTROTHERMAL SIMULATION OF ELECTRIC VEHICLE BATTERY UNDER DRIVING CONDITIONS

Joaquim Manoel Gonçalves
Samuel Luna de Abreu
Luciano Amaury dos Santos
Adriano de Andrade Bresolin
André Luiz Fuerback
Daniel Godoy Costa
Instituto Federal de Santa Catarina, Av. Mauro Ramos, 950 – Centro -CEP 88020-300 – Florianópolis - SC
e-mails: joaquimm@ifsc.edu.br; luciano.santos@ifsc.edu.br; abreu@ifsc.edu.br;
adriano.bresolin@ifsc.edu.br; andre.fuerback@ifsc.edu.br; danielgodoy@ifsc.edu.br

Abstract. *Vehicles that use electric powertrain have become an attractive option for the decarbonization of the world energy matrix. In this scenario, in addition to the car's autonomy, the operating temperature of lithium-ion electric cells requires special attention. In general, cooling is required to remove the heat generated under running conditions, especially in hot climates and during fast charging, while in cold climates heating is required at start-up. This work presents an electrothermal model for the behavior of battery cell temperature coupled to vehicle dynamics to consider its driving conditions as in real rides or standardized test cycles. An analytical expression was obtained for the battery temperature as a function of time with the vehicle traveling in periods of constant speed for a given initial temperature. Experimental tests in chassis dynamometer for a 2013 Nissan Leaf VS vehicle at 22 °C ambient temperature, from an open-source database, were used in the identification of the model parameters. With this model identified and validated, simulation results were obtained and then presented. The systemic approach provided by the developed model ensures agility when used in supporting analysis, design, and control of battery thermal management systems for electric vehicles.*

Keywords: *electric battery thermal management, electric vehicle battery, battery pack temperature, electric vehicle simulation*

1. INTRODUCTION

Lithium-ion batteries (LIB) present a promising solution for powering electric vehicles since they feature high energy density, power density, low self-discharge, and, most important, a long life span. However, under heavy-duty operation in Electric Vehicles (EV) applications, thermal behavior becomes a more delicate issue in battery management. In general, the thermal behavior of a cell is influenced by two factors: the internal factor, namely battery internal parameters, and the external factor, such as drive cycles for example. These two factors determine heat generation within a battery cell, causing temperature rise and in return, these variations may influence battery internal parameters. In long term, the coupled electrothermal relationship defines the operating conditions of the battery cell and the life span. In this work, an electrothermal model is presented and tested for different charging and discharging conditions. This study leads to important conclusions about the significance of each input parameter for future Battery Management System (BMS) implementations and deals with the complexity of the determination of the cell temperature and its impact on the battery pack performance.

The battery internal parameters are approximated based on the electrochemistry within the cell. The models based on Porous Electrode Theory proposed by Doyle et al. (1993) and Single Particle Model by Haran et al. (1998) have been widely used for modeling the dynamic response of LIBs as confirmed by Santhanagopalan et al. (2006). These models show that temperature and current rate are highly involved in the battery dynamics. While electrochemical models have shown the ability to accurately predict the concentration dynamics and terminal voltage, they are characterized by coupled partial differential equations, which overburdens the computation when applied to fast simulation or control design. For this reason, equivalent circuit models are used to simulate electrical behavior. Plett (2004) proposed and compared a series of lumped models. Moreover, different derivatives are proposed to simulate more details in the dynamics, such as hysteresis effects (Hu et al., 2011), Warburg impedance (Kollmeyer et al., 2017), and aging effects (Topan et al., 2016). The present paper focuses on the temperature and current rate dependence of the internal parameters in the context of their electrochemical nature. Previous works are rather profound in shedding light on the energy conversion inside the battery, yet they did not consider the dependence of parameters on temperature and current rate. Thus, they are not suitable for EV applications with heavy-duty drive cycles.

In the case of drive cycles, the cell starts to generate heat due to the electrochemical reactions. Subsequently, the temperature variation caused by heat generation will act on the electrochemical behavior and further influence the thermal behavior. This paper includes the effects of temperature and current rate in the modeling and analysis of lithium-ion cells, giving a more accurate prediction of the electrothermal behavior of the cell. The major achievements can be concluded as follows: (i) The effects of temperature and current rate on the battery internal parameters have been presented and explained based on the electrochemical principles within the LIB. (ii) The model proposed for the study includes these effects and the sensitive coupling relationship between the electrochemical and thermal behaviors of the cell. (iii) Finally, the model is applied to the battery coupled to the vehicle dynamics. The resultant thermal behavior under different drive cycles is compared with real data to prove it can be used to control and improve battery performance.

This paper is organized as follows: Section 2 introduces the proposed model, and its baseline parameter values; section 3 presents the methodology used for model identification, showing the strategies to adjust the parameters using measured data; section 4 analysis the consumption and State of Charge (SoC) of estimates using the model obtained in section 3; section 5 deals with the simulation results; the main conclusions are discussed in section 6.

2. MATHEMATICAL MODEL

The basic idea for the mathematical model is to couple the vehicle dynamics to the battery pack behavior in terms of SoC and temperature variation. Yang et al. (2019) describe a model based on the electrothermal behavior of the batteries under different drive cycles that can be used to improve the battery performance and it is the basis for the following formulation presented in this work. Additional input is given by Miri et al. (2020) that reinforces the need to precisely know the autonomy of an EV.

The model is presented by the equations (1) to (14). This model can compute the cell temperature, in exponential dependence with time, as shown in the analytical solution in the final Eq. (14). The first step is to define the differential equation for the heat balance in the battery as indicated in Eq. (1), with its two terms of heat rates given on the right side.

$$C_{therm} \cdot (dT/dt) = \dot{Q}_{gen} - \dot{Q}_{transf} \tag{1}$$

Where C_{therm} is the thermal capacity of the battery pack of cells ($C_{therm} = n \cdot m \cdot c_p$, where n is the number of cells in the battery pack, m is the mass of one cell and c_p is the equivalent specific heat of the cells), T is the cell temperature, t is the time and $\dot{Q}_{gen}$ and $\dot{Q}_{transf}$ are respectively the heat rate generated inside the cells in operation and the heat rate transferred to the ambient outside of the battery pack. These heat rates can be expressed using Eq. (2) and Eq. (3) as follows.

$$\dot{Q}_{gen} = R_{ohmic} \cdot i^2 + C_{entrop} \cdot i \cdot (T + 273) \tag{2}$$

The generated heat rate in Eq. (2) has two parts: the ohmic and the entropic heat rates in each cell. The ohmic generated heat inside the cells is characterized by its internal ohmic resistance (R_{ohmic}), the entropic heat is characterized by the entropic coefficient (C_{entrop}) and i represents the electrical current flowing through the battery. The entropic coefficient is defined as ($C_{entrop}=dU_{oc}/dT$) the derivative of the cell open-circuit voltage (U_{oc}) in relation to its temperature (Bernardi et al., 1985). In this formulation, the battery discharge electric current has positive values and negative ones during the battery charging. As the entropic heat is released by the battery under positive currents (cooling effect during discharges) and absorbed heat under negative currents (heating effect during charges), the entropic coefficient needs to have a negative value to match this behavior when been multiplied by the electric current as it is in this equation. In this way, the entropic heat is a reversible process, or a regenerative heat with heating and cooling effects, and the ohmic heat is an irreversible one, causing just heating and losses effects.

$$\dot{Q}_{transf} = UA_{pack}.(T - T_{amb}) + \dot{Q}_0 \quad (3)$$

The transferred heat rate in Eq. (3) from all cells in the battery pack to the outside ambient is characterized by its overall thermal conductance (UA_{pack}) which includes all thermal resistances from the temperature of the cells to the outside ambient temperature (T_{amb}) and the term $\dot{Q}_0$ in this equation can be understood as having two origins: to account for any constant heat generated or sunk in Eq. (1) and not yet included in the other terms and also to account for any offset in the temperature difference not completely represented in *(T - T_{amb})*, as there are several pathways for the heat from inside the cells (represented by *T*) to the ambient (represented by T_{amb}) with a varied of temperature differences and thermal resistance to be accounted for.

Table 1. Variables description.

Variable Description	Symbol	Unit
Time	t	s
Cell temperature	T	°C
Outside environment/ambient temperature	T_{amb}	°C
Initial cell temperature	T_{ini}	°C
Coefficient τ in the heat differential equation (Eq. (5))	τ	°C/s
Coefficient η in the heat differential equation (Eq. (6))	η	1/s
Overall battery pack thermal conductance	UA_{pack}	W/°C
Number of cells in the pack	n	/
Mass of one cell	m	kg
Cell average specific heat	c_p	J/kg.°C
Overall battery pack heat capacity ($n.m.c_p$)	C_{therm}	J/°C
Heat rate generated in the cells	Q_{gen}	W
Heat rate transferred between inside and outside the pack	Q_{transf}	W
Cell internal-ohmic electric resistance	R_{ohmic}	Ω
Cell entropic heat coefficient (dU_{oc}/dT)	C_{entrop}	V/°C
Battery pack voltage	U	V
Battery pack open circuit voltage	U_{oc}	V
Electric current in the battery pack	i	A
Electric current in the battery pack due to other electric loads	i_0	A
Road slope angle	α	º
Vehicle mass	M	kg
Factor for the equivalent mass of rotating components	k	/
Gravity acceleration	g	m/s^2
Rolling resistance coefficient	μ	/
Air density (air specific mass)	ρ_{air}	kg/m^3
Vehicle frontal area	A_f	m^2
Vehicle aerodynamic drag coefficient	C_D	/
Mechanical power transmission efficiency	ε	/
Mechanical power transmission efficiency during traction	ε_{drive}	/
Mechanical power transmission efficiency during braking	ε_{regen}	/
Vehicle acceleration	a	m/s^2
Vehicle speed	V	m/s
Time step subscript index	j	/

Then one can put the differential equation given in Eq. (1) to the form expressed in Eq. (4) by rearranging it, using the equations (2) and (3), as follows:

$$dT/dt = \tau - \eta \cdot T \quad (4)$$

Where in Eq. (4):

$$\tau = (R_{ohmic} \cdot i^2 + C_{entrop} \cdot 273 \cdot i + UA_{pack} \cdot T_{amb} - \dot{Q}_0)/C_{therm} \quad (5)$$

$$\eta = (UA_{pack} - C_{entrop} \cdot i)/C_{therm} \quad (6)$$

To find the current (i) present in Eq.(4) the power transmitted from the battery to the car wheel is considered as follows. The electric power consumed by the vehicle motor can be expressed in Eq. (7), where U is the electric voltage of the battery pack.

$$P_{electr} = U \cdot i \tag{7}$$

On the other hand, the mechanical power necessary for its motion is given by Eq. (8), where F is the force in the road contact with the wheels, V is the car velocity, and ε is the powertrain system overall power transmission efficiency.

$$P_{mech} = F \cdot V/\varepsilon \tag{8}$$

The force applied in the road contact for a given velocity (V) and acceleration (a) can be expressed using Eq. (9), where all additional parameters used come from a longitudinal car dynamic model and are listed in Tab. 1, together with all other variables in this mathematical model for nomenclature clarification. This is a general equation for the balance of longitudinal forces acting on a vehicle in motion as the teachings presented by Gillespie, T. D. (1992). This balance of forces has four components: (i) the acceleration responsible for the total variation of vehicle inertia including rotating parts by the k factor; (ii) the component of gravity force (weight) in the longitudinal direction of the displacement; (iii) rolling friction with the road; and (iv) aerodynamic friction with the air.

$$F = k \cdot M \cdot a + M \cdot g \cdot sin(\alpha) + M \cdot g \cdot \mu \cdot cos(\alpha) + C_D \cdot A_f \cdot \rho_{air} \cdot (V - V_w)^2/2 \tag{9}$$

Considering a road with a grade of 0% (α=0°), and zero wind speed ($V_w=0$), Eq. (9) can be expressed in a simplified way as shown in Eq. (10).

$$F = M \cdot (k \cdot a + \mu \cdot g) + C_D \cdot A_f \cdot \rho_{air} \cdot (V^2/2) \tag{10}$$

Considering that the electrical and mechanical powers, expressed in Equations (7) and (8) respectively, are equal, and rearranging them, the electric current can be expressed as shown in Eq. (11), and then two cases can be intuitively deduced from energy flow depicted in Fig. 1. One for forces with positive values, that needs positive currents to drive the vehicle (the red energy flow in Fig. 1), expressed in Eq. (12) with the ε_{drive}, as written in it, lower than one. The second case occurs when the forces have negative values and expressed by Eq. (13) with ε_{regen}, as written in it, higher than one, where mechanical energy is regenerated back into the battery to electric energy again by the negative currents caused by the negative forces (de green energy flow in Fig. 1) acting in the powertrain. In the two cases, there could exist a zero electric current (i_0) all the time due to other electric loads in the vehicle as control systems, electric steering, or the vehicle HVAC system (kept off during the used experimental test).

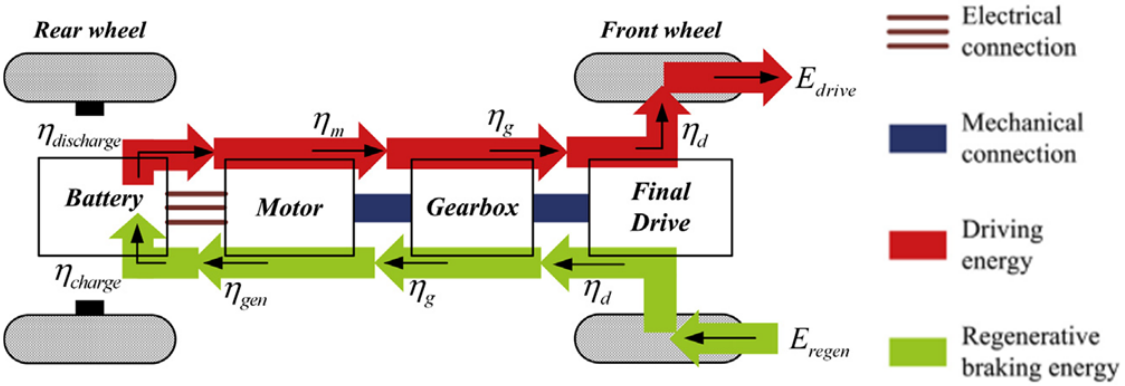

Figure 1. Drive (traction) and regenerative (braking) model representation (adapted from Lv et. al., 2015)

$$i = i_0 + V \cdot F/(U \cdot \varepsilon) \tag{11}$$

$$i_{F>0} = i_0 + V \cdot F/(U \cdot \varepsilon_{drive}) \tag{12}$$

$$i_{F<0} = i_0 + V \cdot F/(U \cdot \varepsilon_{regen}) \tag{13}$$

For the case when the car moves at a constant speed, that means acceleration equal to zero, the differential equation expressed in Eq. (4) has an analytical solution in the format presented in Eq. (14), where the coefficients τ and η are

constants, given by Eq. (5) and Eq. (6) respectively, and with the initial temperature of the cells (T_{ini}) applied as initial condition.

$$T = \tau/\eta + (T_{ini} - \tau/\eta) \cdot e^{-\eta \cdot t} \tag{14}$$

Once the parameters of an actual vehicle are identified, the solution of this model can be computed. The parameters that need to be identified are the following:

- for the electric current, in equations (11), (12) and (13) - i_0, ε_{drive} and ε_{regen};
- for the force, in Eq. (10) - M, and C_D; and
- for the coefficients, in equations (4) and (5) - UA_{pack}, R_{ohmic} and C_{entrop}.

In the next section, it will be shown the identification of these 8 parameters. The others complementary parameters present in the model, such as μ, A_f, ρ_{air}, and g, were imposed using a known constant for them or typical values as in Hayes et al. (2015).

3. MODEL IDENTIFICATION

The identification process needs experimental data. These data are from the D3 (Downloadable Dynamometer Database) and were generated at the Advanced Powertrain Research Facility (APRF) at Argonne National Laboratory (ANL, 2013) under the funding and guidance of the U.S. Department of Energy (DOE). Data is available for 10 vehicles. The published data contained the following variables: elapsed test time (s), speed (mph) and force (N) at the contact of chassis dynamometer and vehicle wheels, battery pack electric current (A) and voltage (V) and SoC (%). In this paper, it was used the data for a 2013 Nissan Leaf SV, in a complete battery discharge at an ambient temperature of 22 °C. The test was performed in March 2014.

The data processing presented here was done with the data filtered in 1 Hz sampling and comparison with values processed with the original 10 Hz sampling has not shown significant differences. The identification was performed using part of the data, the remaining data were used for test and validation of the identified model parameters.

Figure 2 presents the sequence of driving schedules employed, showing the speed that is the main input needed in this identification process. Four different driving schedules were used in this test: UDDS (Urban Driving), HWY (Highway), US06 (United States) and 55mph (55 mph constant speed). The UDDS was repeated four times and the other driving schedules were repeated two times to get the complete discharge of the battery. Data were collected at 10 Hz sampling rate and the complete sequence took almost three hours (9,950 s), which means approximately 100,000 readings for each variable, which corresponds to a range of 144.5 km of displacement distance (Hayes and Davis, 2015).

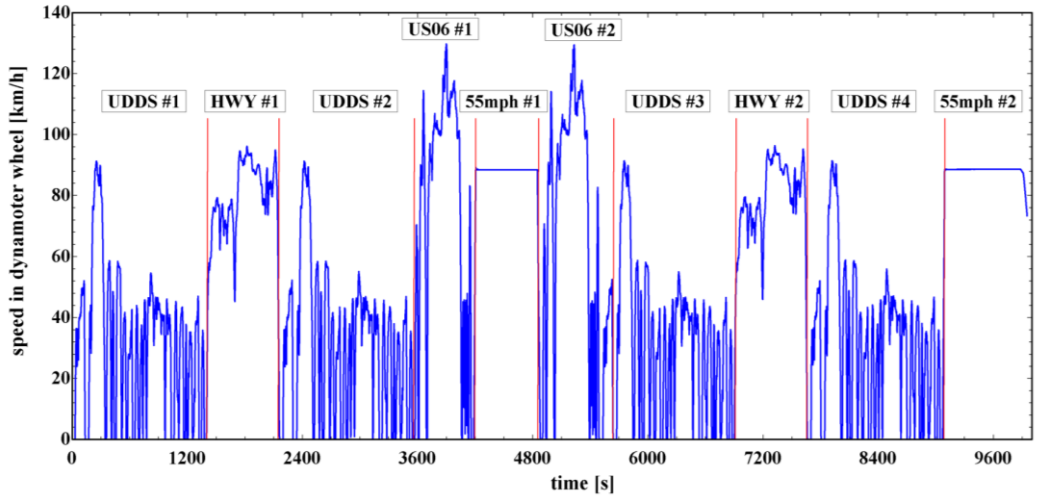

Figure 2. Experimental data from 2013 Nissan Leaf VS during chassis dynamometer test

From the speed, it was calculated the accelerations shown in Fig. 3 in two windows of five minutes of data. During all the tests, variations of the acceleration were typically the ones shown in Fig. 3 within the maximum values of +/- 3.5 m/s^2. Acceleration is computed by Eq. (15), where the subscripts "j" indicates the time step:

$$a_j = (V_j - V_{j-1})/(t_j - t_{j-1}) \tag{15}$$

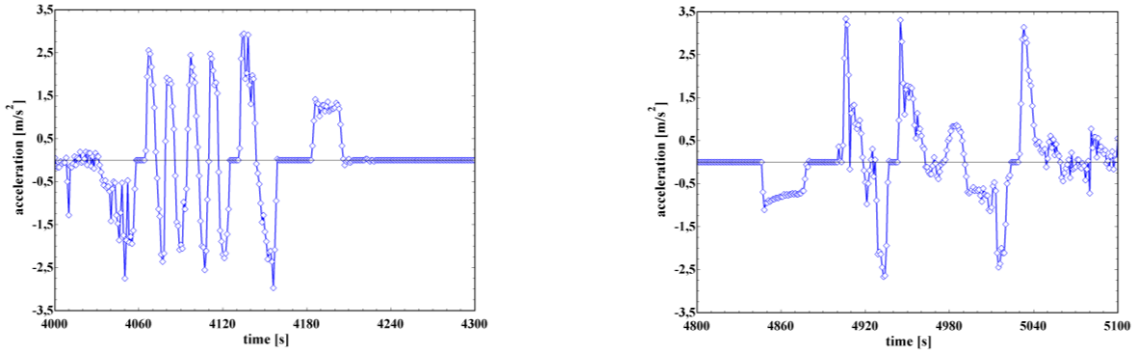

(a) the first calculated acceleration window (b) the second calculated acceleration window

Figure 3. Two windows (of 5 minutes data) of acceleration calculated from measured speed

With the data of force, speed and acceleration the parameters in Eq. (10) were adjusted by the least squares method, and the following values are determined: M = 1,285 kg, C_D = 0.2467. The others complementary parameters are imposed using typical values as: μ = 0,001, A_f =2,27 m^2, ρ_{air} 1.2 kg/m^3 and g = 10 m/s2 (Hayes et al., 2015). The quality of this identification is presented in Fig. 4, where the measured and calculated forces for the same window of Fig. 3(b) are compared..

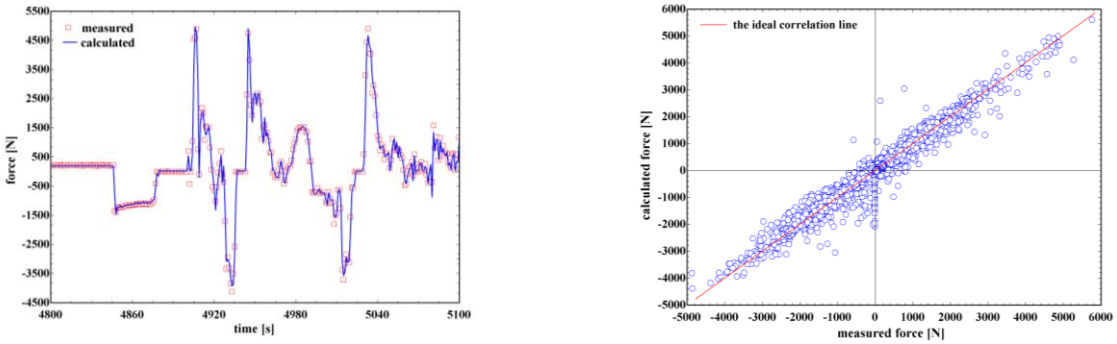

(a) Measured and calculated force versus time (b) Calculated versus measured force

Figure 4. Measured and adjusted force

With the data of electric current and voltage, and with the force calculated by Eq. (10), the parameters in Eq. (12) and (13) were adjusted by the least squares method and the following values were determined: i_0 = 8.685 A, ε_{drive} = 0.8314 and ε_{regen} = 1.048. The quality of this identification is presented in Fig. 5.

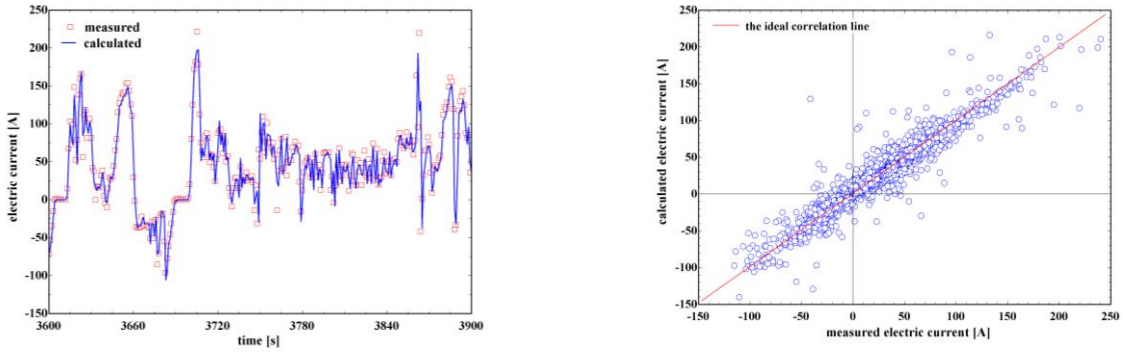

(a) Measured and calculated current versus time (b) Calculated versus measured current

Figure 5. Experimental data from 2012 Nissan Leaf VS in chassis dynamometer test

Using the data of temperature and the calculated electric current the parameters in equations (5) and (6) were adjusted by the least squares method and the following values were determined: UA_{pack} = 70 W/K, C_{entrop} = -73 V/°C, Q_0 = 8932 W and R_{ohmic} = 0.0 Ω. For the others complementary parameters it was used the following imposed values: C_{therm} = 200000 J/°C, T_{amb} = 22 °C.

The quality of this identification process is presented in Fig. 6 and shows a band of errors of maximum +/-1°C for all points in the data considered in this almost 3 hours of test.

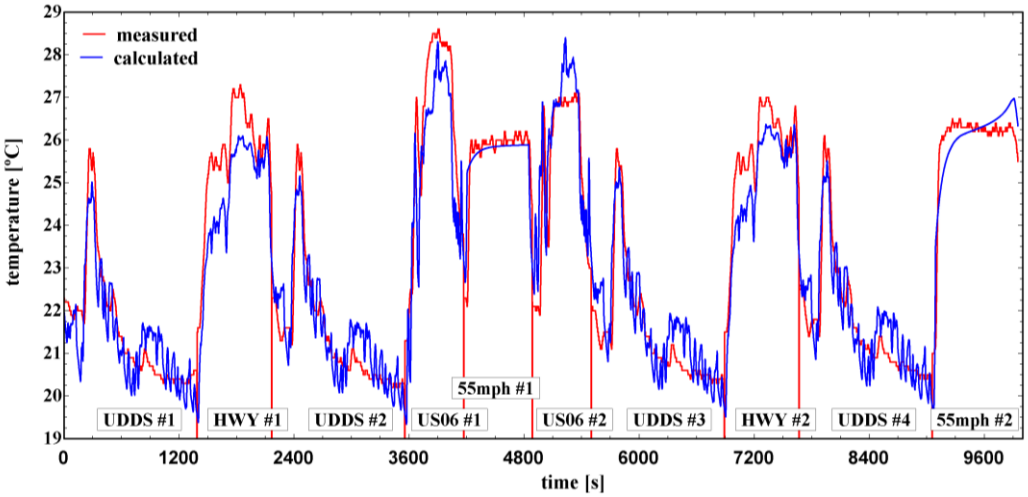

Figure 6. comparison of measured and calculated temperature

The temperature can then be calculated step by step using the analytical solution Eq. (14) as indicated in Eq. (16):

$$T_j = \tau/\eta + (T_{j-1} - \tau/\eta) \cdot e^{-\eta \cdot \Delta t} \tag{16}$$

Alternatively, instead of using the analytical solution, the temperatures can be calculated by direct integrating numerically the differential equation (4). As follows in Eq. (14):

$$T_j = \tau/\eta + (T_{j-1} - \tau/\eta) \cdot e^{-\eta \cdot \Delta t} = \ dT/dt \cdot \Delta t = (\tau - \eta \cdot T_{j-1}) \cdot \Delta t \tag{17}$$

Table 2 summarizes the equations and all parameter values imposed or obtained by the model identification process.

Table 2. Summary of model equations and the values of its parameters.

model equations	parameters values
$F = M \cdot (k \cdot a + \mu \cdot g) + C_D \cdot A_f \cdot \rho_{air} \cdot (V^2/2)$ (10)	M = 1285 kg, k = 1.15, μ = 0.0, g = 10 m/s^2, C_D = 0.2475, A_f = 2.27 m^2, ρair = 1.2 kg/m^3.
$i_{F>0} = i_0 + V \cdot F/(U \cdot \varepsilon_{drive})$ (12) $i_{F<0} = i_0 + V \cdot F/(U \cdot \varepsilon_{regen})$ (13)	i_0 = 8.685 A, ε_{drive} = 0.8314, ε_{regen} = 1.048.
$\tau = (R_{ohmic} \cdot i^2 + C_{entrop} \cdot 273 \cdot i + UA_{pack} \cdot T_{amb} - \dot{Q}_0)/C_{therm}$ (5) $\eta = (UA_{pack} - C_{entrop} \cdot i)/C_{therm}$ (6)	R_{ohmic} = 0.0 Ω, C_{entrop} = -73 V/K, UA_{pack} = 70 W/K, T_{amb} = 22 °C, Q_0 = 8923 W, C_{therm} = 200000 J/K.

4. CONSUMPTION AND SOC ANALYSIS

The vehicle consumption in terms of electric charge (*Ah*), and energy (*E*) in joule, can then be computed by the following numerical integration in time of the electric current, and of the electric power, as expressed by equations (18) and (19), respectively:

$$Ah_j = Ah_{j-1} + i \cdot (\Delta t/3600) \tag{18}$$

$$E_j = E_{j-1} + U \cdot i \cdot \Delta t \tag{19}$$

Also following the same approach, the vehicle range (d), in terms of distance in km, can be computed as expressed by the numerical integration of the speed in time as expressed in Eq. (20) :

$$d_j = d_{j-1} + (V/1000) \cdot \Delta t \tag{20}$$

Knowing the initial SoC (SOC_0), and the battery electric charge at full capacity (Ah_{cap}), the state of charge (SOC) is expressed by Eq. (21), as follows:

$$SOC_j = SOC_0 + 100 \cdot Ah_j / Ah_{cap} \tag{21}$$

In Fig. (7) its is shown the calculated values of SoC and energy consumption as well as the range accomplished during the test. Figure 7(a) compares the SOC provided in the database (D3 from ANL) with the calculated currents after the model identification. For the SoC calculation it was considered 56 Ah as the full capacity and 97 % as the initial state of charge (SOC_0). The results show good agreement, mainly between obtained values. And for the energy consumption shown in Fig. 7(b) it is seen that the energy consumption also follows a similar trend of the vehicle range distance.

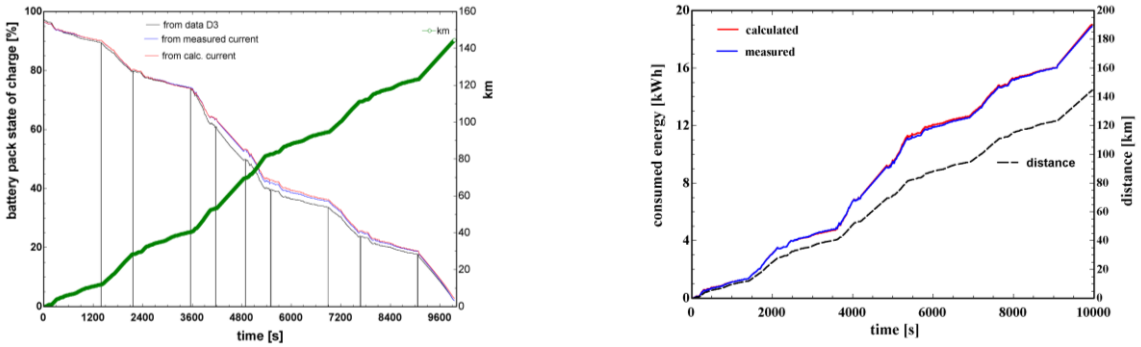

(a) - SoC and range versus time (b) - energy consumption and range versus time

Figure 7. SoC, consumed energy and distance versus time.

5. SIMULATION RESULTS

To perform simulations of the battery thermal behavior with the above model it is also necessary to have the characteristic curve of voltage in relation to SOC (voltage-SOC) for the considered battery. This is needed for computing the electric current by the model with equations (10.2) and (10.3) and in that way also to follow the battery SOC and consumption performance. The electric current equation and the voltage-SOC curve are coupled and need to be solved simultaneously. The voltage characteristic curve was obtained by a least square method using the scaling approach developed by Ahmed M. S.; et. al., (2020) and with the same experimental data from the chassis dynamometer used to develop and to validate the model. In Figure 8 (a) the obtained curve is compared to the experimental data confirming good agreement with the data. The scattering of the measured values of voltage around the curve is mainly due to the temperature variation effect. For the sake of battery thermal behavior simulations, the presented curve was adequate as the following results will show, but it will need improvements if intended for use as an indication of the battery SOC as a function of the measured voltage in actual road conditions. In Figure 8 (b), it is shown simulation results for battery temperature and SOC employing the model with the characteristic curve voltage-SOC for three cases of constant speed rides: 60, 80 and 100 km/h, respectively.

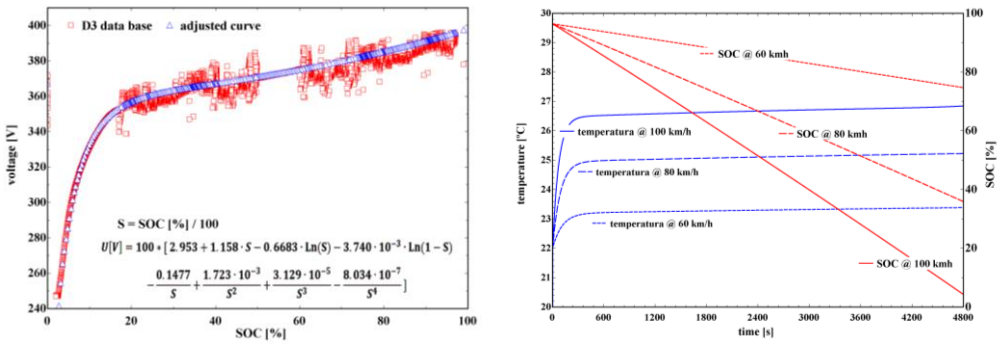

(a) - characteristic curve voltage-SOC (b) - temperature and SOC

Figure 8. Voltage-SOC curve and its simulation results for three constant speed cases

The results for a simulation of a sinusoidal driving schedule are shown in Fig. 9. In this case, the initial speed is the maximum of 100 km/h and varies in a sinusoidal function with a period of 1000 s and a minimum of 60 km/h as it is seen in Fig. 9(a). Also, in the second scale of Fig. 9(a), it is shown the calculated variation of the temperature for this case with a sinusoidal that resulted in a band of +1.5/-1.5 °C around a medium value of 25 °C. The temperature oscillations have a very similar behavior of the speed oscillations in this case, with only around 30 s delay in the periodic regime that follows its approximate 300s of the initial transient regime. In Fig. 9(b) it is seen the comparison of this sinusoidal case (green lines) with the previous constant speeds of maximum (100 km/h), medium (80 km/h) and minimum (60 km/h) values, in terms of temperature (left side scale) and SOC in the second scale (right side scale).

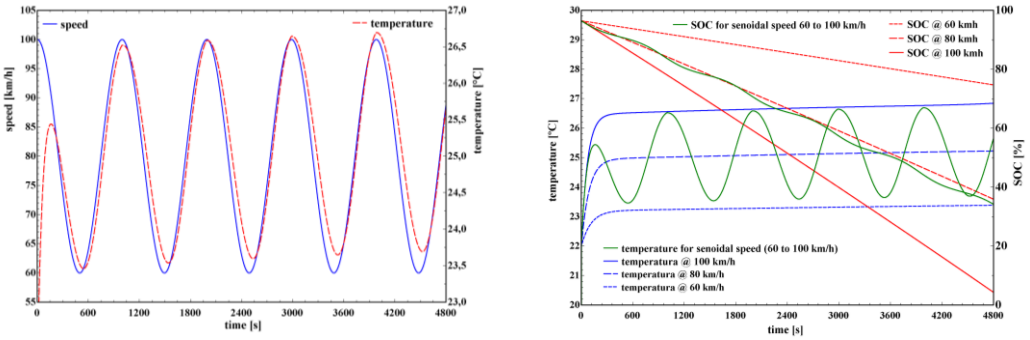

(a) - imposed speed and calculated temperature (b) - comparison of constant x variable speed cases

Figure 9. Simulation results for variable acceleration case (sinusoidal)

6. CONCLUSIONS

The main conclusions of this work are:

- a mathematical model for the thermal behavior of an electric vehicle battery was presented and experimental data were used to identify its parameters. Validation and simulation results were also presented.
- the mathematical model developed is based on fundamental principles with a global approach, represented with lumped parameters of physical significance, such as the overall thermal resistance for the battery heat transfer system.
- the final model consists of three components: the vehicle dynamics; the electric battery and its thermal system for heat transfer between the cells and the external environment.
- for the battery temperature, a differential equation was developed, and its explicit analytical solution was found for the case of constant speed, which allows a better understanding of the parameters involved in the process and helps the model implementation in vehicles in road conditions.
- for a case with acceleration, the differential equation is solved by numerical integration, or in a hybrid way, using the analytical obtained solution for constant speed.
- the parameter identification was performed with experimental data from a chassis dynamometer of a 2013 Nissan Leaf VS at 22°C ambient temperature.
- the final model is composed of four algebraic equations and its identified parameters, that allow a sequential calculation for the following four output variables: (i) vehicle acceleration, (ii) vehicle traction force, (iii) battery electrical current, and (iv) battery temperature.
- the systemic approach provided by the developed model ensures agility when used in supporting analysis, design and control of battery thermal management systems for electric vehicles.
- the presented methodology has strong potential to be used in offline simulations or for online implementation in the electronic hardware of a vehicle BMS for its diagnosis or control.

7. ACKNOWLEDGEMENTS

The authors acknowledge the financial support from ANEEL, CELESC, EMBRAPII and IFSC. The authors are thankful for the collaboration of many colleagues and students, specially Mr. Joao Pereira Pacheco and Mr. Joao Vitor Calazans.

8. REFERENCES

ANL, 2014. “Energy Systems D3 2013 Nissan Leaf SV”, Argonne National Laboratory, 12 Jun. 2022 <https://www.anl.gov/es/energy-systems-d3-2013-nissan-leaf-sv>.

Bernardi, D., Pawlikowski, E. and Newman, J., 1985. “A General Energy Balance for Battery Systems”. J. Electrochem. Soc., Vol. 132, No. 1, pp. 5-12.

Doyle, M., Fuller, T. and Newman, J., 1993. “Modeling of Galvanostatic Charge and Discharge of the Lithium/Polymer/Insertion Cell”. J. Electrochem. Soc., Vol. 140, No. 6, pp. 1526-1533.

Gillespie, T. D. , 1992. Fundamentals of Vehicle Dynamics. SAE International.

Haran, B., White, R., and Popov, B.N., 1998. “Theoretical Analysis of Metal Hydride Electrodes: Studies on Equilibrium Potential and Exchange Current Density”. J. Electrochem. Soc., Vol. 145, No. 12, pp. 4082-4090.

Hayes, J.G. and Davis, K., 2014. “Simplified electric vehicle powertrain model for range and energy consumption based on EPA coastdown parameters and test validation by Argonne National Lab data on the Nissan Leaf”. 2014 IEEE Transportation Electrification Conference and Expo (ITEC). Dearborn, USA, pp. 1-6.

Hu, Y., Yurkovich, S., Guezennec, Y. and Yurkovich, B.J., 2011. “Electrothermal Battery Model Identification for Automotive Applications”. J. Power Sources, Vol. 196, No. 1, pp. 449-457.

Kollmeyer, P., Hackl, A. and Emadi, A., 2017. “Li-Ion Battery Model Performance for Automotive Drive Cycles with Current Pulse and EIS Parameterization”. In Proceedings of the 2017 IEEE Transportation Electrification Conference and Expo (ITEC). Chicago, USA, pp. 486-492.

Lv, C.; Zhang, J., Li, Y., Yuan, Y., 2015. “Mechanism analysis and evaluation methodology of regenerative braking contribution to energy efficiency improvement of electrified vehicles”. Energy Conversion and Management, Vol. 92, pp. 469–482

Miri, I., Fotouchi, A. and Ewin, N., 2020. “Electric vehicle energy consumption modelling and estimation—A case study”. International Journal of Energy Research, Vol. 45, No. 1, pp. 501-520.

Plett, G.L., 2004. “Extended Kalman filtering for battery management systems of LiPB-based HEV battery packs: Part 2. Modeling and identification”. J. Power Sources, Vol. 134, No. 2, pp. 262-276.

Santhanagopalan, S., Guo, Q., Ramadass, P. and White, R., 2006. “Review of Models for Predicting the Cycling Performance of Lithium-Ion Batteries”. J. Power Sources, Vol. 156, No. 2, pp. 620-628.

Topan, P.A., Ramadan, M.N., Fathoni, G., Cahyadi, A.I. and Wahyunggoro, O., 2016. “State of Charge (SOC) and State of Health (SOH) estimation on polymer lithium-polymer battery via Kalman filter”. In Proceedings of the 2nd International Conference on Science and Technology-Computer (ICST). Yogyakarta, Indonesia, pp. 93-96.

Yang, Z., Patil, D. and Babak, F., 2019. “Electrothermal Modeling of Lithium-Ion Batteries for Electric Vehicles”. IEEE Transaction on Vehicular Technology, Vol. 68, No 1, pp. 170-179.

9. RESPONSIBILITY NOTICE

The authors are solely responsible for the printed material included in this paper.